THE AMERICAN MINERALOGIST, VOL. 44, JULY-AUGUST, 1959

# GEOMETRY, ALIGNMENT AND ANGULAR CALIBRATION OF *X*-RAY DIFFRACTOMETERS

W. PARRISH AND K. LOWITZSCH, *Philips Laboratories, Irvington-on-Hudson, New York.*

ABSTRACT

The counter tube *x*-ray diffractometer is widely used both for routine and complicated mineralogical analyses. Very little has been published on the principles and techniques of diffractometry, and consequently many of the instrumental factors which have a profound effect on the data are often overlooked. This paper describes a rapid, precise and reproducible method for the alignment and angular calibration of the goniometer. Simple mechanical devices are employed. The alignment, the zero angle determination to a precision of approximately $\pm 0.001°$ $2\theta$, the precise setting of the 2:1 angular relationship between the receiving slit and the specimen surface and the adjustment of anti-scatter slits can be completed in about one hour. The method makes it possible to achieve optimum performance and to compare data with other diffractometers aligned in the same manner. The geometry, the effects of the more important instrumental and specimen factors, and some performance tests are outlined.

## INTRODUCTION

The increased use of counter tube diffractometers in mineralogical problems has made possible various types of *x*-ray analyses which were difficult or impossible with powder cameras. Although some spectacular results have been achieved with the diffractometer, its full potential has not often been realized. Many factors contribute to the performance, reproducibility and precision of the results. One of these factors is the alignment and angular calibration of the goniometer. In this paper a method that employs simple mechanical devices for rapid and precise alignment and calibration will be described. The instrument and specimen geometrical factors which have a dominant effect on the results obtained with the diffractometer will be outlined.

The diffractometer is obviously a much more complicated instrument than the powder camera and the alignment is therefore correspondingly more difficult. Optimum performance can be achieved only when the goniometer is correctly aligned. Improper alignment may cause a loss of intensity and resolution, distortion of line profiles, increase in background, decrease in peak-to-background ratio and incorrect angle and intensity measurements. The lack of a standard procedure for alignment and calibration causes uncertainty in the results and makes it difficult to compare data with other laboratories or even in the same laboratory.

A few examples will show the difficulties which may be caused by improper alignment. In quantitative analyses of powder mixtures the peak intensities of several lines of the unknown and of a standard substance are measured. If the 2:1 setting is incorrect or different for the

standard and unknown, the peak intensities will be decreased by an amount dependent upon the 2:1 missetting, the absorption and the reflection angle. Since the effect decreases with increasing Bragg angle, the relative intensities will be in error regardless of the statistical accuracy of the counter tube measurements. Good precision in trace analyses requires a minimum background and maximum peak-to-background ratio which can be achieved only with correct alignment. In the study of clay minerals the disorder stacking of the silica sheets and the particle size may be obtained from Fourier analysis of the line profiles. If the line profiles are distorted because of incorrect alignment as well as from the diffraction effects, the separation of the two is practically impossible. In precision measurements of lattice parameters and interplanar spacings for indexing low symmetry substances, accurate angular calibration is essential to achieve the required precision. In qualitative analyses of mixtures and low symmetry substances, good resolution is required to minimize overlapping. There are many more examples that could be cited.

Of course there are other factors in addition to alignment that must be considered to achieve optimum performance, but these will not be described here. The reader may consult the literature on the use of counter tube methods (Parrish and Kohler, 1956); intensity measurement techniques and counting statistics (Parrish, 1956; Mack and Spielberg, 1958); specimen crystallite size statistics (Klug and Alexander, 1954; de Wolff, Taylor and Parrish, 1959), and instrumental aberrations (Parrish and Wilson, 1959; Parrish, 1959b).

*X-ray Protection*

It is essential in making the alignment to be particularly careful to avoid exposure to the *x*-ray beam. Since the procedure involves some manipulation of devices without the benefit of all the radiation protective features, caution should be exercised and temporary radiation shields should be used as required. The diffractometer counter tube may be used to survey the set-up (Kohler and Parrish, 1956).

## Goniometer Alignment

The conditions that must be realized for correct alignment can be obtained from a study of Fig. 1. The axis of rotation of the goniometer should lie midway between the line focus of the *x*-ray tube, which is used as the geometrical source, and the receiving slit. The long axes (*Z*-direction) of the *x*-ray tube line focus, divergence, receiving and anti-scatter slits must have a common median line, be parallel to each other and to the goniometer axis of rotation *O*, and lie in the *YZ*-plane when the detector is at 0°. The metal foils of the parallel or Soller slits must lie in planes normal to the *Z*-axis.

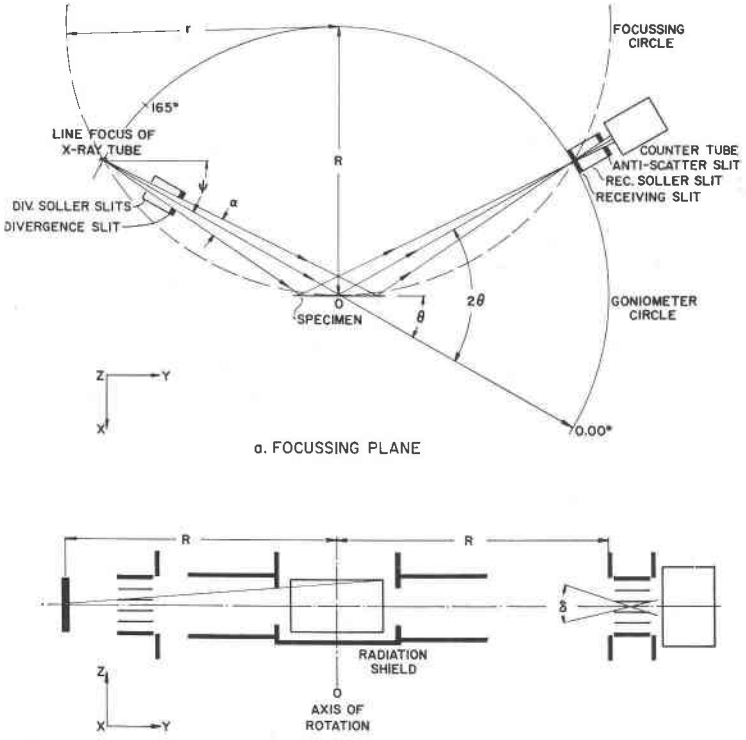


FIG. 1. Geometry of the diffractometer in the focussing plane (above) and axial plane (below). $R$ radius of goniometer, $r$ radius of focussing circle, $O$ goniometer axis of rotation, $\psi$ angle of view of target, $\alpha$ full angular aperture in focussing plane, $\delta$ angle aperture limited by Soller slits. The orthogonal coordinate system $XYZ$ is used to facilitate descriptions.

The angle-of-view of the $x$-ray tube target surface, $\psi$, is defined with respect to the ray that passes through $O$. A divergent beam is used and the zero angle of the goniometer scale is defined with respect to the $\psi$-angle. The 2:1 (receiving slit: specimen surface scanning relationship) setting is made with respect to the zero angle.

The distance between the target and mounting surfaces may vary slightly from one tube to another, and if this occurs $\psi$ will also vary slightly. Although small changes in $\psi$ do not change the resolution, they do require a recalibration of the zero angle and consequently the 2:1 setting. The procedure described below makes it easy to allow for such variations. Care must be taken to avoid tilting the axis of the $x$-ray tube with respect to the mounting surface of the tube shield.

If the focal spot of the $x$-ray tube is rotated with respect to the window,

or the plane of the target surface is not perpendicular to the long axis of the tube, the projected size of the line focus accordingly will be increased or decreased. This alignment and projected size can be checked by establishing a reference line from pinhole images of both spot focus windows and then making a pinhole image of the line focus at a known magnification. Normally this is not done unless the construction of the tube is believed to be faulty.

Drawings of the alignment and calibration devices are shown in Fig. 2. Although these devices have been designed for the Norelco goniometer (Parrish, Hamacher and Lowitzsch, 1954), the same principles are applicable to other goniometers. The dimensions of the devices permit direct alignment of the goniometer simply by matching one surface against another. The only critical dimension is the height of $D$ in the $X$-direction, which must be the same as the height of the slit and horizontal line on the

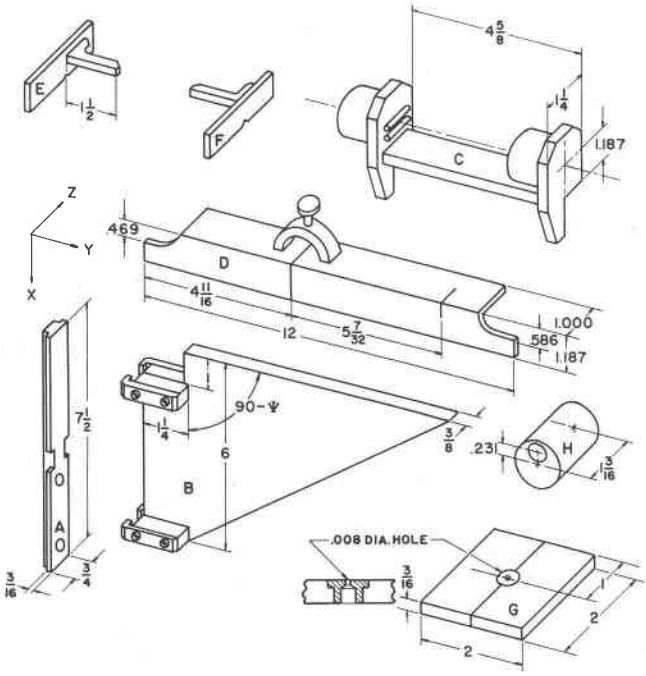


FIG. 2. Mechanical devices designed for alignment and calibration of Norelco goniometer. $A$ bar mounted on $x$-ray tube tower, $B$ machined $\psi$-angle surface, $C$ slit and fluorescent screen which clips on $B$ to set $\psi$, $D$ alignment device which sets in specimen holder, $E$ and $F$ fixtures set in divergence and receiving slit positions, $G$ pinhole and flat plate for zero angle calibration and 2:1 setting, $H$ bushing with off-center hole for elevating divergence Soller slit assembly for $\psi = 6°$.

fluorescent screen above the mounting surface of $C$. These devices can be easily duplicated with ordinary machine shop facilities.

*Preliminary Alignments*

Several preliminary steps are required before proceeding to the final alignment. Normally these are done only when making an installation for the first time, or when major modifications are made. It is good practice to adjust the $x$-ray unit so that the table is horizontal.

Bar $A$ is permanently screwed to the middle of the face of the $x$-ray tube tower with its long axis perpendicular to the top surface as shown in Fig. 3. This mounting may be facilitated by removing the $x$-ray tube and using a machinist's square on the top surface of the tower.

The alignment of the elements of the goniometer itself (slit assemblies and goniometer axis) is accomplished with devices $D$, $E$, and $F$. Device $D$ should be mounted on the specimen post with its reference line coinciding with the reference line of the specimen post (Fig. 3b). $D$ must rest straight against the back surface of the post to avoid a rotation in the $YZ$-plane. The clamp holding the specimen post is loosened so that the post can be rotated freely (but not translated in the $Z$-direction); the counter tube arm is set at approximately 0° and $D$ is rotated until its left side strikes the bottom of the divergence slit assembly. $E$ and $F$ are inserted and this may require a small angular movement of the counter tube arm. The divergence and receiving slit posts are then rotated until the arms of $E$ and $F$ lie evenly on the top surface of $D$ ($YZ$-plane).

The position of the receiving Soller slit assembly in the direction parallel to $Z$ is fixed with respect to the counter tube arm and should not be changed. Furthermore, the goniometer is constructed so that the long axes of the divergence and receiving slit assemblies ($Z$-direction) are parallel to each other and to the goniometer axis of rotation. The specimen post and divergence Soller slit assembly should be translated along $Z$ until the front surfaces of arms $E$ and $F$ are flush with the front surface of $D$ in the $XY$-plane. When the arms of $E$ and $F$ are flush with the top and front surfaces of $D$, the divergence, receiving, and antiscatter slits have a common median line which intersects and is normal to the goniometer axis of rotation. If the tip of arm $F$ does not coincide with the reference mark on $D$, the receiving Soller slit assembly should be translated along $Y$ to set $R=17$ cm. The Soller slit assemblies should then be locked, $E$ and $F$ removed, and the specimen post with $D$ still mounted on it should be slipped out of the goniometer.

*Setting Angle-of-View*

The triangular device $B$ is placed on $A$ as shown in Fig. 3(a). $B$ has been machined so that the top surface is inclined by the desired $\psi$-angle. $C$ consists of a narrow horizontal slit in the front (left) and a flat plastic fluorescent screen in the back (right). $C$ is clipped on $B$, which is moved vertically on bar $A$ by means of a thumb screw until the image of the $x$-ray tube focal spot appears centered on the horizontal line in the middle of the fluorescent screen.* $B$ is then locked in position with the other thumb screw and $C$ is removed. The top surface of $B$ is now at the correct height for device $D$.

*Goniometer Position*

The goniometer must now be aligned with respect to the $x$-ray tube. The screws on the under side of the $x$-ray table that hold the goniometer locating plate should be loosened to allow free movement of the goniometer. The front two levelling screws are set in the locat-

* An alternative procedure is to remove the fluorescent screen, use the second slit (right side of $C$) and a stationary counter tube.

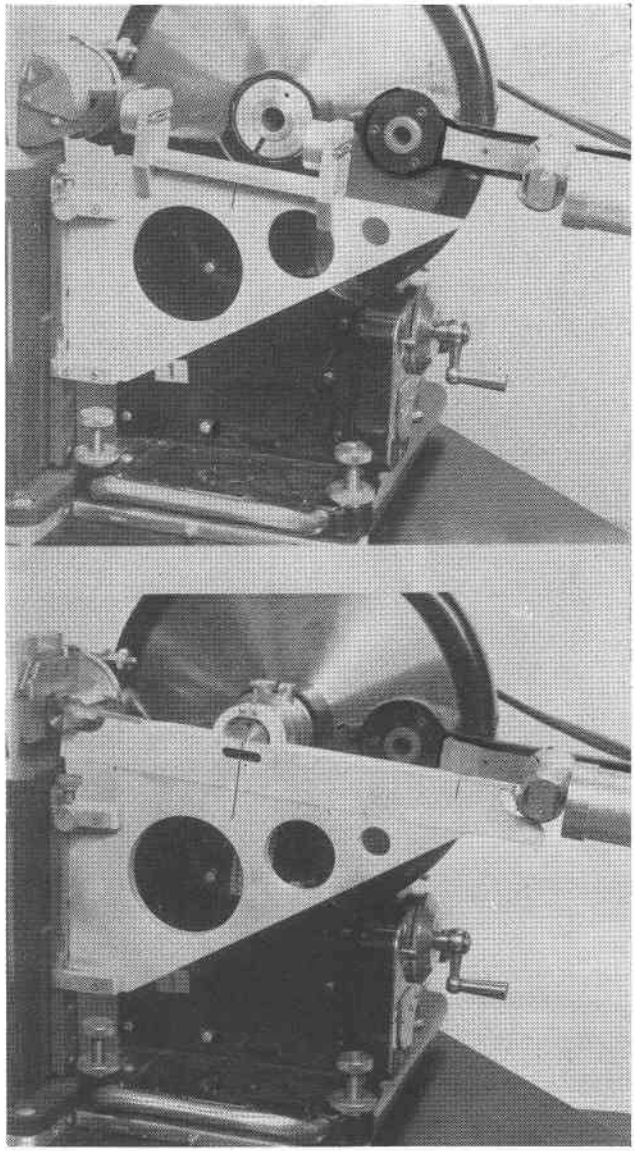

FIG. 3. (*a*) The $\psi$-angle is obtained by clipping $C$ on $B$ and moving $B$ vertically on $A$ until the image of line focus of the $x$-ray tube appears centered on the fluorescent screen on $C$. (*b*) The goniometer alignment is made by moving the goniometer to match $B$ and $D$. (See Fig. 2.)

ing plate. The distance of $O$ above the table top must be made large enough (by rotating the levelling screws) to allow the reinsertion of $D$ and the specimen post as shown in Fig. 3(b). Three adjustments of the goniometer position must then be made: (1) The goniometer (and locating plate) are moved on the $x$-ray table until the reference line on $D$ matches that on $B$; this sets $O$ to the correct distance in front of the focal line of the $x$-ray tube so that the focal line lies on the goniometer circle. (2) The levelling screws are adjusted so that the bottom surface of $D$ touches the top surface of $B$; this sets $O$ at the correct height for the selected $\psi$-angle. (3) The levelling screws are readjusted until the front surfaces of $D$ and $B$ are flush in the $XY$-plane (check with a straight-edge); this aligns the position and direction of the median line of the goniometer with respect to the focal line of the $x$-ray tube.

In practice it is usually necessary to repeat these three steps a few times because step 3 may alter the settings of the levelling screws made in step 2. There should be no appreciable contact pressure between $D$ and $B$. $E$ and $F$ may be reinserted to make certain the front surfaces of their arms are flush with the front surface of $D$ in the $XY$-plane. The levelling screws and locating plate are then tightened. $D$, $E$ and $F$ are removed, but $B$ is left in place for the angular calibration. The goniometer alignment can usually be completed in less than one-half hour.

*Centering the Primary Beam*

If in the construction of the divergence slit, the opening was not accurately centered, the procedure described above may not give a precise centering of the primary beam on the specimen. The centering of the beam may be checked with the $x$-ray tube operating at full power and a *flat* ruled fluorescent screen in the specimen post. Since a divergent beam and extended flat specimen are used, the primary beam can be centered exactly only at some chosen angle. In scanning to other angles the geometrical center of the beam will gradually change with respect to $O$. For example, if the 1° divergence slit is rotated to center the beam on the fluorescent screen which has been set normal to the incident beam, the latter will appear off-center by about 1 mm. when the screen is set for $2\theta = 20°$.

It is generally desirable in routine work to center the beam with the screen set at the lowest scanning angle to be used, particularly when working at small angles, say $\theta < 10°$, because here the length of specimen illuminated increases rapidly with a small decrease in $\theta$. This procedure eliminates scatter which may occur from the primary beam striking the ends of the specimen holder. It should also be noted that the centering of the primary beam may vary among several divergence slits if the distances between the middle of the opening and the reference edge are different.

The distribution of intensity across the specimen in the $Z$-direction may be observed by looking down on a fluorescent screen mounted in the specimen holder with the specimen radiation shield in place. The angle at which this is done is not important, but the primary $x$-ray beam intensity should be sufficiently small (say 25 kV, 10 ma) that variations of the fluorescent intensity are discernible. The front and back edges of the screen in the $Z$-direction will appear to be slightly less strongly illuminated because of the way the divergent rays overlap in passing through the divergence Soller slit. The brighter strip of illumination should appear centered on the screen. If it is to one side, the focal spot of the $x$-ray tube may be improperly oriented or mis-centered, there may be a cutoff at the window of the $x$-ray tube housing, or the divergence Soller slit assembly may be inclined from its proper position normal to the $Z$-direction.

## Angular Calibration

Several methods have been used for calibrating the angular scale of the goniometer. The most common method has been to use a "standard"

substance whose lattice parameter has been accurately determined by some other $x$-ray instrument, usually a powder camera, to construct a calibration curve. The limitations of this method will be described below. In the mechanical method the 0° angle is accurately measured and it is assumed that the gear system accurately moves the receiving slit-counter tube arm to the angle indicated on the scale. If desired, the angular precision of the gear train can be checked to about one second of arc by use of precision polygons (Taylerson, 1947; Haven and Strang, 1953). The equipment required for this purpose is expensive and specialized techniques are used for the calibration.

*Mechanical Method*

This method is based upon determining the 0° angle with respect to the ray that makes the desired $\psi$-angle with the target surface and passes through the goniometer axis of rotation and center of the receiving slit. The procedure is done with $x$-rays, but it does not require reflection from a specimen and hence is not subject to systematic errors. It may be applied with a fine slit, pinhole (Parrish, Hamacher and Lowitzsch, 1954), or a knife edge (Tournarie, 1954), and is far more accurate than the other methods described below. The principle is illustrated in the ray diagram and observed intensity distributions in Fig. 4. The anti-scatter slit should be removed and the $x$-ray machine and circuits operated for about an hour with full power on the $x$-ray tube to make certain that equilibrium conditions have been reached before making the calibration.

The $\frac{5}{8}$ in. diameter rod of the specimen post must fit snugly into the goniometer because loose fitting will cause an error in the calibration by approximately twice the amount of clearance (measured on an angular scale). The use of the calibrating slit requires the removal of the specimen post, but use of the flat plate with fine pin-hole ($\approx 0.008$ in. diameter) or knife edge does not. The three calibration devices should give the same results, but there are some advantages in the use of the pinhole. The intensities are considerably lower (and hence less filtering is required) than for the slit or knife edge. In addition, the pinhole device is also used to make the 2:1 setting, whereas the other devices cannot be used for this purpose. There may be some confusion in the use of the knife edge. In Fig. 4, all rays up to the dotted line will pass through the upper half of the divergence slit, but beyond the dotted line the intensity falls off giving a sloping line similar in appearance to the calibration line. The angle at which this occurs depends upon the angular aperture $\alpha$. For example, with $\alpha = 1°$ it occurs at approximately 0.5° $2\theta$ from the 0° position.

The pinhole plate is set in the specimen holder with the pinhole ap-

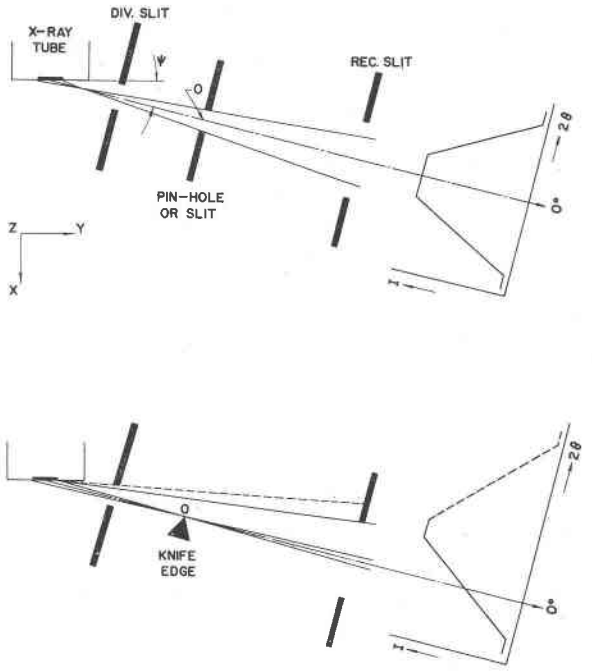


FIG. 4. Schematic ray diagram of 0° calibration using pinhole or slit (above) and knife edge (below). The intensity distributions are on the right.

proximately aligned on the axis of rotation (middle of the specimen post) and the large surface of the plate normal to the selected central ray as shown in Fig. 4. A small machinist's square set on top of $B$ may be used to make the setting, which, although not critical, should be approximately correct in order to obtain the same intensities for the following two series of measurements. One series is made with the plate in this position and another series is made after the specimen holder (with pinhole plate) is rotated 180°. The pinhole plate must not be moved with respect to the specimen holder from its original clamped position.

The intensity distributions are measured by step-scanning in 0.01° steps using either manual settings or step gears (Parrish, Hamacher and Lowitzsch, 1954; Parrish, 1956; Hamacher and Lowitzsch, 1956). To avoid backlash errors, the distribution should always be scanned in the same direction; the counter tube arm should be moved manually in this direction for a few tenths of a degree before beginning the recording at the base of the peak. The intensities must be measured with good statistical accuracy. A simple method is to continuously drive the step gears and record with the ratemeter using a 2 sec. time constant. It takes

30 secs. for the drive gears on the goniometer to make one revolution so that about 28 secs. is spent at each step.

The counting rates should be kept low enough to avoid the necessity of non-linearity corrections for counter or circuit resolving time. In the case of full-wave rectified operation of a copper target tube operated at about 15 kVp, 7 ma, $\psi = 6°$, 0.0025 in. nickel filter, 1° divergence slit and 0.006 in. receiving slit, the observed peak intensity is about $4 \times 10^3$ counts per sec. with a scintillation counter without pulse amplitude discrimination. If a Geiger counter is used the filtering should be increased to reduce the peak counting rate to about 500 counts per sec. By using a low voltage on the $x$-ray tube nearly all the radiation measured has about the same wavelength as CuK$\alpha$. If higher voltages were used, greater filtering would be required and the radiation measured would consist largely of considerably shorter wavelengths.

The data from the recordings may be plotted as shown in Fig. 5. The median line (dashed) of each set of readings is constructed and the line (dot-dash) lying midway between the two median lines is the 0.00° position. Since both distributions are symmetrical, the median lines are vertical. The angular separation of the two sets of readings will depend on how closely the pinhole was aligned with the axis of rotation; the separation should not exceed about 0.2°. The 0.01° dial may be set to the measured zero angle or a correction may be applied to all future readings.

The 0° angle can also be derived from the knife edge data as shown in Fig. 5 (right). The two sets of data for the 180° rotation are symmetrical, and the vertical median line is easily constructed from the midpoints.

Using the procedure outlined above, it is possible to determine the zero angle position to a precision of about $\pm 0.001°$ in about one-half hour. By manual setting on the peaks of the pinhole curves, a precision of $\pm 0.01°$ may be obtained in a few minutes.

*Effect of Receiving Slit on Calibration*

The greater the height of the receiving slit (in the $X$-direction), the broader the curves obtained with the pinhole and the less steep the knife edge curves. Both methods give the same answer when the *same* receiving slit is used. However, if the $X$-distance between the central longitudinal line of the receiving slit and the reference edge (Fig. 5 insert) varies from one slit to another, the derived zero angle will also vary. For example, two different 0.006 in. receiving slits were used to determine the data used in Fig. 5 and gave zero angles, 0.003° apart, because $X$ was not the same in both slits. Furthermore, if the $X$-distance of the 0.018 in. receiving slit had been the same as that of the 0.006 in. slit, the zero angles derived from both also would have been the same. Since it is difficult to achieve the mechanical tolerances required to obtain exactly the same zero angle calibration with different receiving slits, a separate calibration should be made for each receiving slit.

It should be noted that the receiving slit height has a major role in determining the resolution, intensity and peak-to-background ratio (Parrish, 1956). The narrower the slit,

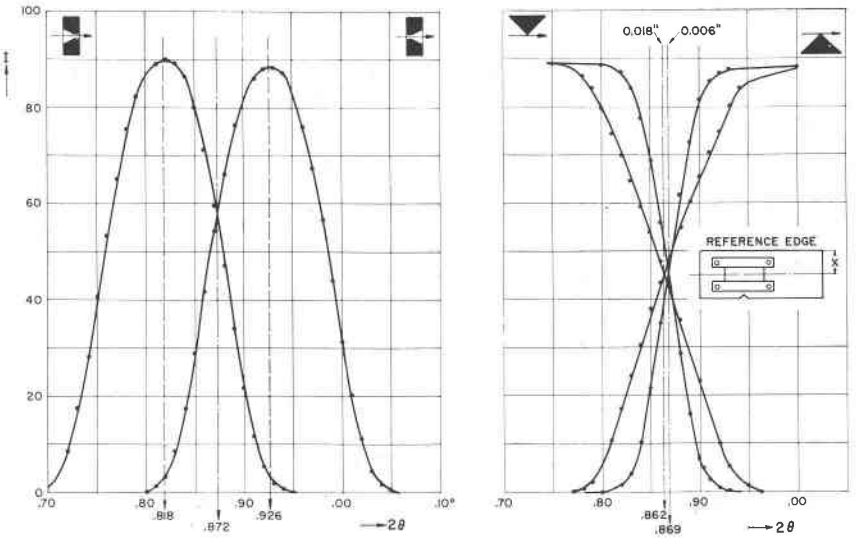


FIG. 5. Plot of data to determine 0° angle using pinhole (left) and knife edge (right).

down to about 0.003 in., the greater the resolution and the lower the intensity. However, aside from its effect on the observed K$\alpha$-doublet overlap, the receiving slit height causes only symmetrical broadening, whereas other instrumental aberrations cause asymmetric broadening and shifts in the line positions.

*4θ-Method*

Another method for determining the zero angle is to measure the $2\theta$-angles of a number of reflections on both side of the 0° position. This method is equivalent to measuring $4\theta$ in powder camera calibrations; it has been used for a long time and has recently been described as the Cornu method (Neff, 1956). It requires setting the 2:1 relationship (see below) *before* making the calibration. It also requires the specimen holder be temporarily disengaged from the goniometer, rotated exactly 180°, and then reengaged before scanning to obtain the reflection below 0°. Any error in the 180° rotation causes an incorrect 2:1 setting which broadens the line, shifts the peak and thereby introduces a random error. The angular positions of a number of reflections must be measured above and below 0° and averaged. The precision of the determination is limited by the random errors in the individual measurements and it also requires much longer time than the mechanical method.

## *Use of Standards*

Frequently a specimen of a "standard" substance whose lattice parameter has been established by other methods is used for angular calibration. The reflection angles $2\theta_{cal}$ are calculated and a graph is drawn relating the observed angles of the standard, $2\theta_{obs}$ or $2\theta_{obs} - 2\theta_{cal}$ to the calculated values. The unknown substance is then measured under the

same experimental conditions, and its $2\theta_{obs}$ values are corrected by means of the calibration curve.

Assumptions which are implicit in this procedure are that the random errors in the measurement of the standard are negligible and that the systematic errors (Parrish and Wilson, 1959; Parrish, 1956b) will be the same for both the standard and unknown. Thus it must be assumed that the standard and unknown are both perfect specimens, that the specimen surface displacement error is the same for both, and that both have the same absorption. It is also clear that the precision of the method cannot exceed the precision with which the lattice parameter of the standard has been determined. In fact, good practice in physical measurements requires that the reflection angles of the calibration substance be known with considerably better precision than is required in the measurement of the unknown. Unfortunately, there is now considerable doubt that the accuracy attainable in precision lattice parameter measurements exceeds about 0.013% (Parrish, 1959a). Nevertheless, standards are useful in assessing the performance of the equipment. Reflection angles and recordings for diamond, silicon and tungsten and other substances for several $x$-ray wave lengths are given elsewhere (Parrish and Mack, 1959). The line profiles of well-crystallized standards are required to check the resolution, peak-to-background ratio, intensity, and similar factors as described at the end of this paper.

Some of the uncertainties that arise from the use of standards may be circumvented by using an internal standard (Chayes and MacKenzie, 1957; Swanson, Gilfrich and Cook, 1957). A small amount of the standard substance is intimately blended with the unknown, and the measurements of $2\theta_{obs}$ of the standard and $2\theta_{obs}$ of the unknown are then made on the same specimen. This procedure may reduce the errors from differences in specimen surface displacement, but most of the difficulties remain. In addition, the standard adds more, although known, lines to the pattern.

It should be clear that when the zero angle calibration is made by the mechanical method, the peak positions of the lines of a standard substance show deviations from the calculated values by amounts dependent upon the systematic and random errors in the measurements.

## Specimen Surface Displacement and Transparency

Displacement of the specimen surface from the goniometer axis of rotation is the common source of many relatively large systematic errors in angular measurements. If the specimen surface is displaced a distance $x_{s.d.}$ from $O$, the observed reflection angle is shifted (Wilson, 1950) by an amount

$$\Delta(^\circ 2\theta)_{s.d.} = 114.5916\, x_{s.d.} \cos\theta/R.$$

A plot of this expression for various values of $x_{s.d.}$ is shown in Fig. 6. The shift is toward higher angles if the specimen surface is inside the focussing circle or toward lower angles if it is outside. The entire line profile is shifted, and thus the formula applies to the peak, median, center-of-gravity* or other measures of the line position.

This displacement error may be caused by non-coincidence of the reference surface of the goniometer specimen holder with $O$, and in this

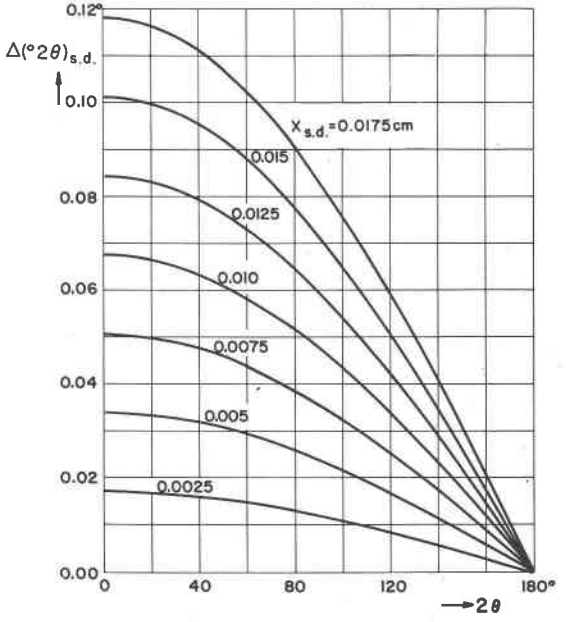


FIG. 6. Angular error caused by specimen surface displacement.

case readings on all specimens will be in error by a constant amount at a given angle. The surface of the holder should be checked with respect to the $\frac{5}{8}$ in. diameter rod with a precision dial indicator gauge, surface plate and gauge blocks. If the errors are caused by poor specimen preparation, or failure to shim the mounting surface when using slide smear preparations, the errors will vary from one specimen to another. The calibration procedures described above do not take these types of errors into account and they must be treated separately. (See also Parrish, 1959b.)

Unless the shift is extremely large, the shape of the line profile and the intensity are unchanged.

* The center-of-gravity $\tilde{\theta}$ is defined as $\tilde{\theta} = \int\theta f\theta d\theta / \int f(\theta) d\theta$; see Ladell, Parrish and Taylor (1957, 1959).

A somewhat similar error will arise if the specimen has a low linear absorption coefficient $\mu$, because some of the diffraction will take place below the specimen surface. This transparency error always shifts the lines to smaller angles and causes asymmetric broadening of the lines. The shift of the center-of-gravity of a line $\Delta(2\theta)_{tr}$ (expressed in radians) is

$$\Delta(2\theta)_{tr} = \frac{\sin 2\theta}{2\mu R} - \frac{2x_t \cos\theta}{R\,[\exp(2\mu\, x_t \csc\theta) - 1]}$$

where $x_t$ is the specimen thickness. If the beam is completely absorbed in a thick absorbing specimen, $\mu\, x_t \csc\theta$ is large and the second term may be dropped. The shift thus increases with decreasing $\mu$, is maximum at 90° ($2\theta$) and zero at 0° and 180°. Some typical values of $\Delta(2\theta)_{tr}$ at 90°($2\theta$) for $R = 17$ cm. expressed in degrees are: 0.067° for $\mu = 25$ cm$^{-1}$, 0.017° for $\mu = 100$ cm$^{-1}$, 0.002° for $\mu = 1000$ cm$^{-1}$. In the case of negligible absorption of the beam in a thin transparent specimen, the expression becomes

$$\Delta(2\theta)_{tr} = x_t \cos\theta / R$$

(expressed in radians).

## 2:1 Setting

To obtain proper focussing conditions, the counter tube must be set at twice the angle of the specimen with respect to the 0° ray, and this 2:1 relationship must be maintained at all reflection angles by an accurate tracking arrangement. Deviations from the correct 2:1 setting cause line broadening and a decrease of peak intensity. Also, if other misalignments are present they may combine with 2:1 missetting to cause a shift of the line. The magnitude of these effects increases with decreasing $2\theta$, which causes further errors in the relative peak intensities and line-breadths. In measurements of line profiles and peak intensities and small Bragg angles, such as are required in clay mineral studies, an incorrect 2:1 setting will have a profound effect on the results (Parrish, 1959b).

A powder specimen in the reflecting position is frequently used to set the 2:1. This method has the disadvantage of being relatively insensitive to small missettings. A single crystal plate might be used to make this setting, but this requires that the atomic reflecting plane be exactly parallel to the surface of the crystal and that a very narrow incident ray be accurately centered on the axis of rotation.

A mechanical method of precisely setting the 2:1 at 0° is recommended. It is assumed that the goniometer gears will maintain this relationship at all angles. A long slit, a double knife edge or a flat plate* may be used, as illustrated in Fig. 7. The $x$-ray intensity should be some-

* To avoid total reflection at grazing incidence, the surface should not be highly polished.

what reduced from that used for the 0° calibration by the addition of more filters. The 2:1 setting must be made with the goniometer locked in the previously determined 0.00° position. One of the three devices is placed in the specimen holder and the latter is rotated until maximum intensity is obtained. The correct 2:1 position is sharply defined because even a slight rotation of the order of 0.01° will cause a large decrease of intensity. The specimen holder is locked in this position while the count-

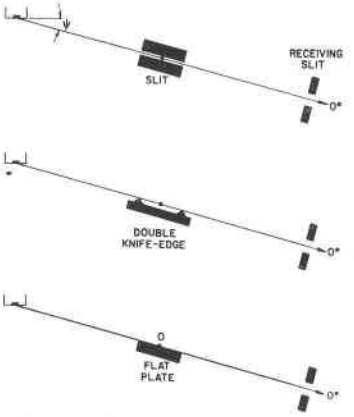


FIG. 7. Methods for 2:1 setting at 0°.

ing rate is observed on the rate-meter to make certain that the locking has not changed the 2:1 setting.

A new device, shown in Fig. 8, facilitates the accurate setting of the 2:1 position. It consists of two arms operated in scissor fashion by a micrometer screw about 4 in. from the axis of rotation, and it is spring loaded to give a positive action and to allow adjustments from either direction. One full turn of the micrometer screw rotates the specimen post 0.03°. The device may be mounted on the specimen post or on the rear of the goniometer. The later placement is desirable when temperature chambers, helium path, etc., are to be used.

When the rotating specimen holder (Parrish, 1956) is employed, the devices described above are not used and the 2:1 setting is made by use of a slot about $\frac{1}{4}$ in. wide and 0.001 in. deep milled across the median line on top of the holder. With the counter tube at 0.00°, the holder is rotated to the position of maximum intensity and locked in the same manner as described above.

## ANTI-SCATTER SLITS

A low, nearly uniform background can be obtained by the proper use of anti-scatter slits. The receiving slit and the anti-scatter slit in front

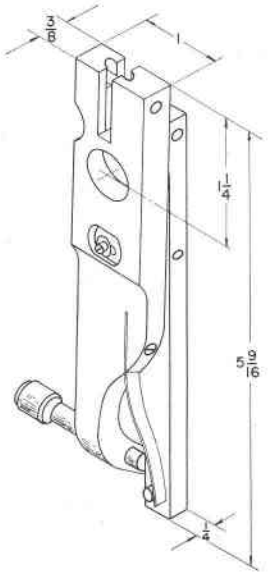


FIG. 8. Precision 2:1 adjustment device. The dimensions are in inches.

of the counter tube together limit the radiation which enters the counter tube to only that radiation scattered from the length of the specimen illuminated in the $Y$-direction. The air scatter is thereby also reduced to a minimum. The $X$-dimension of the anti-scatter slit opening is made slightly larger than the $X$-dimension of the beam at this position. This may be calculated from the angular aperture $\alpha$ and the $X$-dimension of the receiving slit. The anti-scatter slit is aligned by slowly rotating it around the $Z$-direction until the peak intensity of a strong reflection from a good specimen is observed to be maximum. The peak intensity should remain nearly the same when the slit is removed. If the intensity increases markedly (say $>2\%$) when the slit is removed, the alignment is incorrect or the slit height is too small.

The slot in the internal cylinder of the specimen radiation shield also reduces extraneous scatter by preventing primary $x$-rays from striking beyond the 1 cm. width ($Z$-direction) of the specimen as shown in the lower left side of Fig. 1. For specimens 1 cm. wide, Soller slits with full aperture $\delta=4.5°$, and $R=17$ cm., the slot should be 0.85 cm. wide. It is essential that the median line of the slot coincide with the median line of the specimen.

The front of the specimen radiation shield facing the $x$-ray tube may scatter $x$-rays into the counter tube at high reflection angles. The internal

cylindrical shield which contains the slot is $2\frac{1}{8}$ in. diameter, and above about 140° $2\theta$ the background begins to rise slightly because of scatter from the metal. If the diameter of the cylinder with the slot is increased to 5 in., the increase of background from metal scattering will be apparent only above about 170° $2\theta$. If the larger diameter is used the slot must be made narrower or a wider specimen used to avoid scatter from the specimen holder in the $Z$-direction as explained above.

### Angle-of-View of Target

Normally a small angle-of-view ($\psi=3°$) of the target surface has been used to obtain a small projected height of the $x$-ray tube line focus (Parrish and Hamacher, 1952). It has recently been found that the projected height can be increased by a factor of two without decreasing the resolution (Parrish, 1958). Since the intensity is zero at grazing incidence and increases with increasing $\psi$ at a rate dependent upon the voltage, atomic member of the target element and smoothness of the target surface, the intensity may be increased about 25% by increasing $\psi$ from 3° to 6° for a given set of experimental conditions. For a given aperture $\alpha$, the primary intensity along the $Y$-dimension of the specimen also becomes more uniform at larger $\psi$.

In high precision diffractometry it is preferable to set the center-of-gravity of the primary $x$-ray beam intensity distribution rather than the geometrical center on the axis of rotation (Wilson, 1954). The center-of-gravity remains fixed at all angles and the effects of certain instrumental misalignments are minimized. The geometrical center and center-of-gravity differ by an amount dependent upon the distribution of intensity in the primary beam. With a copper target $x$-ray tube operated at 40 kVp, $\alpha=4°$ and $\psi=3.0°$, the center-of-gravity is at 3.3°. For the same conditions except that $\psi=6.0°$, the center-of-gravity is at 6.06° which is so close to the geometrical center that the latter may be used.

In the case of the Norelco goniometer, increasing $\psi$ from 3° to 6° decreases the upper limit of the scanning range from 165° to 162° $2\theta$, and several minor modifications are required. A collar $\frac{1}{2}$ in. high should be inserted at the base of the $x$-ray tube tower to raise the $x$-ray tube tower window. The lower part of the window opening in the tower may also have to be enlarged. The divergence Soller slit assembly must be raised, and an easy way of doing this is to make a bushing (Fig. 2H) which fits into the boss that holds the assembly. The right side of the Soller slit assembly is also turned down to fit into the $\frac{3}{8}$ in. hole of the bushing. Another bushing with a centered hole can be used with the same assembly at $\psi=3°$. The alignment procedure is exactly the same as for $\psi=3°$, but the top surface of the triangular fixture $B$ must be machined at 6°.

### Alignment for Single Crystals

When either large flat single crystal plates or small crystals for structure work are to be studied, certain modifications in the procedure are required. The goniometer alignment and zero angle setting are made with a 1° divergence slit and 0.006 in. receiving slit according to the procedure described above. With the counter tube locked in the zero angle position, the pinhole is manually translated small distances in the specimen holder (*keeping fingers out of the beam*) until successive 180° rotations cause no variation of intensity, which indicates that the hole is centered on the goniometer axis of rotation. A smaller divergence slit, say $\alpha=1/12°$, is then centered by noting the maximum intensity transmitted by the centered pinhole. The smaller divergence slit is required to reduce the intensity to measurable limits, to illuminate only the narrow region around the axis of rotation, and to prevent

"walking" of the reflected beam from a large plate during rotation (the latter would cause errors in the relative intensities at different angles if the reflecting power varied along the crystal surface.) The 2:1 setting is made with the crystal by adjusting the precision 2:1 device to obtain maximum intensity while the goniometer is slowly scanning in the region of the wide peak of the continuous radiation (around 8°–10°2$\theta$ at 40 kVp). This technique avoids possible small changes in the 2:1 setting which might occur when the clutch is engaged. Finally, the narrow receiving slit is replaced by a wide receiving slit of the order of 1 mm. in the $X$-direction to make the recording less sensitive to slightly erratic movements of the gear train, which would cause large intensity variations in single crystal measurements. The total intensity may be greatly reduced by the insertion of pinholes or lead stops on the divergence and receiving slits to limit their lengths in the $Z$-direction.

### Mechanical Tests

It is assumed that the divisions on the dial which read to 0.01° are accurately engraved. For precision work the divisions should be checked against an accurately engraved scale by standard precision machine ship procedures.

The uniformity of movements of the counter tube, the 2:1 gear tracking, and the backlash may be checked as follows: A large range dial indicator gauge which is sensitive to 0.0001 in. is mounted on the base of the goniometer and its contact point placed against the bottom of the receiving slit assembly when the gauge is in about the middle of its range. When the goniometer arm is driven at a slow speed ($\frac{1}{8}$° per min.) the motion of the arm can be seen on the gauge and erratic movements readily observed. The goniometer arm is driven down scale to any selected gauge reading and the corresponding 0.01° dial reading noted. Scanning should be continued about 0.1° beyond this point, the scanning direction reversed and the goniometer driven to the same gauge reading where another reading of the 0.01° dial is made. The difference between the two dial readings is a measure of the backlash. To check the uniformity and backlash of the 2:1 tracking, the contact point of the dial indicator gauge is placed against a rigid bar about 6 in. long mounted on the specimen post. These checks should be repeated at several positions in the scanning range of the goniometer.

To obtain reproducible readings it is essential that the reference edge of the slits (top) be flat and parallel to the median line of the slit opening. If the two sides of the slit opening are not parallel, various aberrations may be introduced. If two slits have the same nominal height in the $X$-direction but do not in fact have *exactly* the same opening, the intensity and resolution will vary accordingly. It is usually satisfactory to measure the effects of the differences for some standard conditions so that the proper corrections can be made if required. Other consequences of imperfect slit construction were pointed out in the section on angular calibration.

There are several points to check in the recorder system. The angle-marking pen records 0.5°(2$\theta$) increments on the chart. If necessary the microswitch on the 0.01° dial must be adjusted so that it operates exactly at the 0.00° and 0.50° positions. The chart pen on the recorder must ink a line parallel to the chart grid when the chart is not in motion. This can be checked by turning the chart drive motor off and manually moving the pen by means of the knurled drive inside the recorder. The directions for calibrating and checking the electronic circuits and detector are beyond the scope of this paper.

## $X$-ray Results

The recordings in Fig. 9 show the type of results that may be obtained with a properly aligned diffractometer. Quartz was used as an example

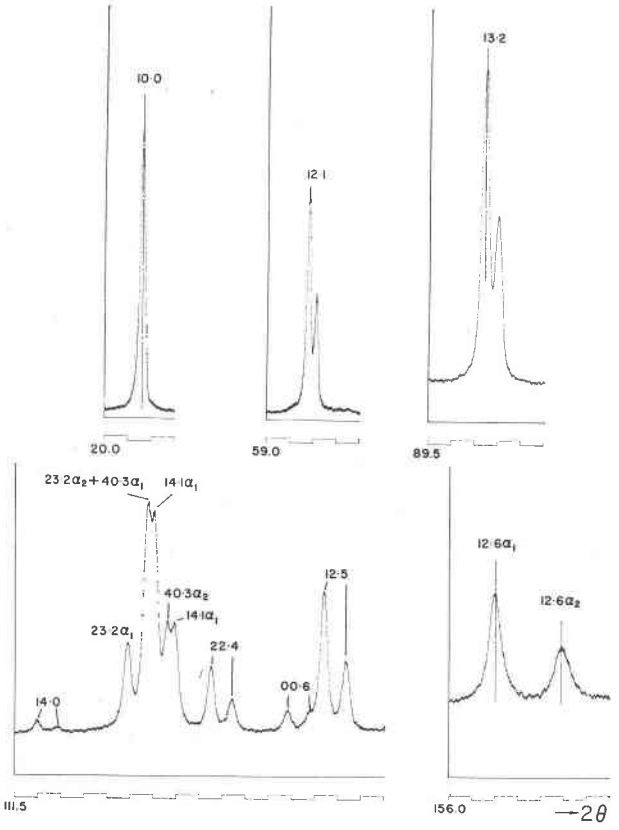


FIG. 9. Recordings of portion of quartz powder pattern. Rotating specimen, $<20\mu$ crystallites, CuK, 40 kVp, 20 ma, 0.0007 in. Ni filter, $\psi=6°$, scintillation counter with pulse amplitude discrimination, 2 sets of Soller slits each with $\delta=4.5°$, scanning speed $1/8°(2\theta)$ per min., scale factor 32 (full scale=1600 counts per sec.) for all recordings except 12·1 where scale factor was 16.

| *hk·l* | 10·0 | 12·1 | 13·2 | 12·5 | 12·6 |
|---|---|---|---|---|---|
| Ang. Ap. $\alpha$ (deg.) | 1 | 1 | 4 | 4 | 4 |
| Rec. Slit (in.) | 0.003 | 0.003 | 0.012 | 0.012 | 0.012 |
| Time Constant (sec.) | 4 | 4 | 8 | 8 | 8 |
| P-B (counts/sec.) | 1022 | 389 | 1116 | 483 | 360 |
| (P-B)/B | 45 | 35 | 8 | 3 | 1 |
| Backg. meas. at (°$2\theta$) | 19.0 | 58.5 | 92.0 | 119.5 | 156.0 |
| Width (°$2\theta$, (P-B)/2) | 0.18 | 0.12 | 0.20 | 0.20 | $0.31_6$ |

because it is ideally suited for such tests and is widely available. A powder with crystallites $<20\mu$ was prepared from a large Brazilian crystal of oscillator-plate quality. The powder was mixed with a small

amount of binder (1 vol. collodion diluted with 10 vol. amyl acetate), packed in a flat holder for a rotating specimen, and after drying, the top surface was scraped flush with the reference rim. The experimental conditions are described in the caption of Fig. 9.

The $x$-ray tube had been used about 5000 hours, and it is likely that somewhat higher intensities would have been obtained with a newer tube. The intensity data were obtained from manual settings on the $K\alpha_1$ peaks and the backgrounds were read at the angles indicated. The intensities with Geiger counters or proportional counters would be about one-half the values obtained with the scintillation counter because of their lower quantum counting efficiencies (Taylor and Parrish, 1955). The backgrounds would be higher if pulse-amplitude discrimination had not been used (Parrish and Kohler, 1956). In the present case the window of the pulse-height analyzer was set symmetrically around the average pulse amplitude for CuK$\alpha$ to detect about 93% of CuK$\alpha$.

In the description of the results given below, it should be noted that if a recording which matches only one of those shown in Fig. 9 is obtained, this is not sufficient evidence that the instrument is properly aligned. Similar results must be obtained for several reflections over the entire scanning range to be certain the alignment is correct. The complex of lines appearing in the region 111° to 119° ($2\theta$) serve as a good measure of the overall performance. The small intensity of the $14\cdot0\alpha_1$ line is clearly visible above background although the peak-to-background ratio is only 0.3. The three lines $23\cdot2$, $14\cdot1$ and $40\cdot3$ each with $K\alpha_1$–$K\alpha_2$ components are resolved except for $23\cdot2\alpha_2$ and $40\cdot3\alpha_1$ where the separation is only 0.034° ($2\theta$). The $00\cdot6\alpha_2$ line is partially resolved from the base of $12\cdot5\alpha_1$.

The line profiles of well-crystallized specimens obtained with even a properly aligned diffractometer are not symmetrical. They are asymmetrically broadened and shifted by various aberrations inherent in the geometry of the instrument. Some of these, such as specimen surface displacement, specimen transparency, receiving slit height, and 2:1 missetting have been mentioned above. The effects of a few of the other aberrations will be briefly described so that the nature of the profiles may be better understood. Practically all the aberrations have been analyzed and experimentally confirmed (Wilson, 1950; Parrish and Wilson, 1959; Parrish, 1959b).

The flat specimen aberration is caused by the use of a flat specimen rather than one whose curvature varies continuously during scanning to match the focussing circle. It causes a shift in the center-of-gravity of the reflection to smaller angles (the peak also shifts by an amount which is smaller but much more difficult to calculate) by an amount

$$\Delta(^\circ 2\theta)_{f.s.} = (\alpha^2 \cot \theta)/343.7748.$$

This error is zero at 180° $2\theta$ and increases with decreasing $2\theta$-angle. Some typical values of the shift are 0.008° ($\alpha = 4°$, $2\theta = 160°$), 0.046° ($\alpha = 4°$, $2\theta = 90°$), 0.003° ($\alpha = 1°$, $2\theta = 90°$), 0.016° ($\alpha = 1°$, $2\theta = 20°$). The reason for the asymmetric broadening and the greater shift of the center-of-gravity than of the peak is that the high-$2\theta$ side of the reflection remains nearly fixed but the low $2\theta$-side, particularly the lower part, is stretched toward smaller $2\theta$-angles.

The axial ("vertical") divergence (Pike, 1957) also asymmetrically broadens and shifts the line, toward lower angles below 100°$2\theta$ and toward higher angles above 100°$2\theta$. The shift of the center-of-gravity is given by the expression

$$\Delta(^\circ 2\theta)_{a.d.} = 0.01125 \cot 2\theta + 0.00188 \csc 2\theta$$

for two sets of Soller slits and the instrumental parameters of the Norelco goniometer. Some typical values of the shift are: −0.074° (10°$2\theta$), −0.012° (45°$2\theta$), +0.011° (140°$2\theta$), and +0.035° (165°$2\theta$).

The asymmetry and shift may be reduced by decreasing the apertures $\alpha$ and $\delta$ but only at the expense of a large loss of intensity. All the aberrations "fold" (convolute) with each other and require rather elaborate mathematical unfolding procedures to determine each of the separate effects. However, the centers-of-gravity of the aberrations are additive. For example, the shift of the center-of-gravity of the 10·0 line is: flat specimen (−0.016°) + transparency (−0.008°) + axial divergence (−0.036°) = 0.060°$2\theta$. The asymmetry of this line is evident particularly in the lower portion of the low-$2\theta$ side of the profile. This additive property and the fact that the aberrations are not known in terms of the shift of the peak are the principle reasons for using the center-of-gravity rather than the peak angle in high precision measurements (Ladell, Parrish and Taylor, 1957, 1959).

The width of the partially resolved CuK$\alpha_1$ lines in the front-reflection region using an aperture $\alpha = 1°$ and 0.003 in. receiving slit varies from 0.10° to 0.12° ($2\theta$) measured at one-half peak height above background. The width depends on the degree of overlapping of the K$\alpha$-doublet lines and the instrumental aberrations, and is smaller at the larger reflection angles. When the aperture $\alpha$ is increased from 1° to 4° and the receiving slit from 0.003 in. to 0.012 in. to obtain greater intensity in the back-reflection region, the line breadth of the 13·2 reflection is doubled, the peak intensity increased by a factor of 12, and the peak-to-background ratio decreased from 9·5 to 7·8. Although the axial divergence effect is small in this region, the flat specimen aberration is large and the line is asymmetrically broadened. The line symmetry may be restored by

using a smaller aperture $\alpha$, but this would cause a reduction in the intensity.

In the far back-reflection region (above about 140°), the contributions to the line breadth and position of all the aberrations except axial divergence becomes less important. However, the dispersion increases rapidly in this region and the lines become broader because the primary $x$-rays are not strictly monochromatic. In fact, the intensity distributions of the $x$-ray spectral lines are generally asymmetric, and the degree of asymmetry and the breadth vary among the lines from the same target as well as from one target element to another (Bearden and Shaw, 1935). The Lorentz and polarization factors and the dispersion increase so rapidly in this region that they cause a distortion of the line profile and contribute significantly to the breadth and asymmetry. These effects can be seen in Fig. 9 in which the 12·6 CuK$\alpha_1$ line is $0.31_5°$ wide and the 12·6 CuK$\alpha_2$ line is $0.36_2°$ wide (Ladell *et al.*, 1959).

## References


Bearden, J. A. and Shaw, C. H. (1935), Shapes and wavelengths of $K$ series lines of elements Ti 22 to Ge 32: *Phys. Rev.*, **48,** 18–30.

Chayes, F. and Mackenzie, W. S. (1957), Experimental error in determining certain peak locations and distances between peaks in $x$-ray diffractometer patterns: *Am. Mineral.*, **42,** 534–547.

de Wolff, P. M., Taylor, J. M. and Parrish, W. (1959), Experimental study of effect of crystallite size statistics on $x$-ray diffractometer intensities: *J. Appl. Phys.*, **30,** 63–69.

Hamacher, E. A. and Lowitzsch, K. (1956), The "Norelco" counting-rate computer: *Philips Tech. Rev.*, **17,** 249–254.

Haven, C. E. and Strang, A. G. (1953), Assembled polygon for the calibration of angle blocks: *J. Research Natl. Bur. Standards*, **50,** 45–50.

Klug, H. P. and Alexander, L. E. (1954), *X*-ray Diffraction Procedures: John Wiley & Sons, Inc., New York.

Kohler, T. R. and Parrish, W. (1956), Conversion of quantum counting rate to Roentgens: *Rev. Sci. Instr.*, **27,** 705–706.

Ladell, J., Parrish, W. and Taylor, J. (1957), Measurement and use of the center-of-gravity of line profiles in $x$-ray powder diffractometry: *Am. Cryst. Assoc.*, Pittsburgh meeting, Nov. 8, 1957, Paper No. 46; Parrish, W. and Taylor, J. (1957), The precision diffractometer measurement of lattice parameters: *Acta Cryst.*, **10,** 741.

Ladell, J , Parrish, W. and Taylor, J. (1959), Center-of-gravity method of precision lattice parameter determination: *Acta Cryst.*, **12,** 253–254; Interpretation of diffractometer line profiles: *ibid.*, **12** (in press); Dispersion, Lorentz and polarization effects in the centroid method of precision lattice parameter determination: *ibid.*, **12,** (in press).

Mack, M. and Spielberg, N. (1958), Statistical factors in $x$-ray intensity measurements: *Spectrochim. Acta*, **12,** 169–178.

Neff, Hans (1956), Über die präzisionsbestimmung von gitterkonstanten mit dem zählrohr-interferenz-goniometer: *Zeit. f. ang. Phys.*, **10,** 505–507.

Parrish, W. (1956), *X*-ray intensity measurements with counter tubes: *Philips Tech. Rev.*, **17,** 206–221.

PARRISH, W. (1958), Optimum *x*-ray tube focal spot geometry for powder diffractometry: *Am. Cryst. Assoc.*, Milwaukee meeting, June 24, Paper No. G-8, p. 35.

PARRISH, W. (1959a), Precision measurement of lattice parameters of polycrystalline specimens: (I.U.Cr. Apparatus Commission Report) *Acta Cryst.* (in preparation).

PARRISH, W. (1959b), Advances in *x*-ray diffractometry of clay minerals: *Proc. Seventh Natl. Conf. Clays and Clay Minerals*, Washington, 1958, Pergamon Press, Inc., New York. In press.

PARRISH, W. AND HAMACHER, E. A. (1952), Geiger counter *x*-ray spectrometer: instrumentation and techniques: *Trans. Inst. and Meas. Conf., Stockholm*, 95–105.

PARRISH, W., HAMACHER, E. A. AND LOWITZSCH, K. (1954), The "Norelco" diffractometer: *Philips Tech. Rev.*, **16,** 123–133.

PARRISH, W. AND KOHLER, T. R. (1956), Use of counter tubes in *x*-ray analysis: *Rev. Sci. Instr.*, **27,** 795–808.

PARRISH, W. AND MACK, M. (1959), *X*-ray reflection angle tables: (In preparation.)

PARRISH, W. AND WILSON, A. J. C. (1959), Precision measurement of lattice parameters of polycrystalline specimens, Int. Tables for *X*-Ray Cryst.: vol. 2 (216–234).

PIKE, E. R. (1957), Counter diffractometer—The effect of vertical divergence on the displacement and breadth of power diffraction lines: *J. Sci. Instr.*, **34,** 355–363; *ibid.*, **36,** 52–53.

SWANSON, H. E., GILFRICH, N. T. AND COOK, M. I. (1957), Standard *x*-ray diffraction powder patterns: Natl. Bur. Standards Circular 539.

TAYLERSON, C. O. (1947), Testing circular division by means of precision polygons: *The Machinist* (London), **71,** 1821–1824.

TAYLOR, J. AND PARRISH, W. (1955), Absorption and counting efficiency data for *x*-ray detectors: *Rev. Sci. Instr.*, **26,** 367–373, *ibid.*, **27,** 108.

TOURNARIE, M. (1954), Reglage absolu d'un goniometre a compteur de Geiger-Müller: *J. Phys. et Radium*, **15,** Supp. No. 1, 11A–15A.

WILSON, A. J. C. (1950), Geiger counter *x*-ray spectrometer-influence of size and absorption coefficient of specimen on position and shape of powder diffraction maxima: *J. Sci. Instr.*, **27,** 321–325.

WILSON, A. J. C. (1954), A theoretical re-investigation of geometrical factors affecting line profiles in counter diffractometry, distributed at 3rd I.U.Cr., Paris; abstract: PARRISH, W. AND WILSON, A. J. C. (1954), *Acta Cryst.*, **7,** 622.

*Manuscript received November 11, 1958.*